Z. Phys. C – Particles and Fields 41, 385–393 (1988)

Zeitschrift für Physik C Particles and Fields

Evidence for direct photons from quarks in electron-positron annihilation

TASSO Collaboration

W. Braunschweig, R. Gerhards, F.J. Kirschfink, H.-U. Martyn

I. Physikalisches Institut der RWTH Aachen, Federal Republic of Germany[a]

B. Bock[1], H.M. Fischer, H. Hartmann, J. Hartmann, E. Hilger, A. Jocksch, R. Wedemeyer

Physikalisches Institut der Universität Bonn, Federal Republic of Germany[a]

B. Foster, A.J. Martin, A.J. Sephton

H.H. Wills Physics Laboratory, University of Bristol, Bristol, UK[b]

F. Barreiro[2], E. Bernardi[3], J. Chwastowski[4], A. Eskreys[5], K. Gather, K. Genser[6], H. Hultschig, P. Joos, H. Kowalski, A. Ladage, B. Löhr, D. Lüke, P. Mättig[7], D. Notz, J.M. Pawlak[8], K.-U. Pösnecker, E. Ros, D. Trines, T. Tymieniecka[6], R. Walczak[6], G. Wolf

Deutsches Elektronen-Synchrotron DESY, Hamburg, Federal Republic of Germany

H. Kolanoski

Institut für Physik, Universität Dortmund, Federal Republic of Germany[a]

W. Gerhardt, T. Kracht[9], J. Krüger, E. Lohrmann, G. Poelz, P. Rehders, G. Tysarczyk[10], W. Zeuner

II. Institut für Experimentalphysik der Universität Hamburg, Federal Republic of Germany[a]

J. Hassard, J. Shulman, D. Su

Department of Physics, Imperial College, London, UK[b]

A. Leites, J. del Peso

Universidad Autonoma de Madrid, Madrid, Spain[c]

C. Balkwill, M.G.Bowler, P.N. Burrows, G.P. Heath, P. Ratoff, I. Silvester, I.R. Tomalin, M.E. Veitch

Department of Nuclear Physics, Oxford University, Oxford, UK[b]

G.E. Forden[11], J.C. Hart, D.H. Saxon

Rutherford Appleton Laboratory, Chilton, Didcot, UK[b]

S. Brandt, M. Holder, L. Labarga[12]

Fachbereich Physik der Universität-Gesamthochschule, Siegen, Federal Republic of Germany[a]

Y. Eisenberg, U. Karshon, G. Mikenberg, A. Montag, D. Revel, E. Ronat, A. Shapira, N. Wainer, G. Yekutieli

Weizmann Institute, Rehovot, Israel[d]

D. Muller, S. Ritz, D. Strom[13], M. Takashima, Sau Lan Wu, G. Zobernig

Department of Physics, University of Wisconsin, Madison, Wis., USA[e]

Received 29 July 1988

[1] Now at Krupp Atlas Elektr. GmbH, Bremen, FRG
[2] Alexander v. Humboldt Fellow, on leave from Universidad Autonoma de Madrid
[3] Now at Robert Bosch GmbH, Schwieberdingen, FRG
[4] On leave from Inst. of Nuclear Physics, Cracow, Poland
[5] Now at Inst. of Nuclear Physics, Cracow, Poland
[6] Now at Warsaw University, Poland
[7] Now at IPP Canada, Carleton University, Ottowa, Canada
[8] On leave from Warsaw University[f], Poland
[9] Now at Hasylab, DESY
[10] Now at University of Heidelberg, Heidelberg, FRG
[11] Now at SUNY Stony Brook, Stony Brook, NY, USA
[12] Now at SLAC, Stanford, CA, USA
[13] Now at University of Chicago, Chicago, IL, USA

[a] Supported by Bundesministerium für Forschung und Technologie
[b] Supported by UK Science and Engineering Research Council
[c] Supported by CAICYT
[d] Supported by the Minerva Gesellschaft für Forschung GmbH
[e] Supported by US Dept. of Energy, contract DE-AC02-76ER000881 and by US Nat. Sci. Foundation Grant number INT-8313994 for travel
[f] Partially supported by grant CPBP 01.06

Abstract. Hadronic events from e^+e^--annihilations with a high energy isolated photon have been investigated at C.M. energies between 14 GeV and 44 GeV. A forward-backward asymmetry A_γ of the positively charged jet with respect to the incident positron direction has been found: $A_{\gamma\gamma} = -0.32 \pm 0.07$, providing evidence for photon bremsstrahlung from quarks. The forward-backward asymmetry of all hadronic events at C.M. energies between 30 GeV and 36 GeV has been measured. The value, corrected for the limited polar angle acceptance of the detector, is: $A = +0.021 \pm 0.005$.

1 Introduction

Direct photon emission from quarks is a powerful tool to explore various properties of the quarks and the hadronization mechanism [1–3]. If the photon is e.g. radiated at very short quark distances it is a signal from the time before fragmentation takes places.

Because of the electromagnetic coupling of direct photons to quarks, they can be used to probe the electric charge of the quarks. The most commonly used quark model assumes for the electric charges of the quarks $-1/3$ or $2/3$ independent of their colour, whereas the gluons are assumed to be neutral. Although this model is in agreement with all experimental results it is not the only way to build a consistent picture of the hadrons. There are competitive models, first proposed by Han and Nambu, which assume integer charged quarks, whose different colour states have different electric charges [4].

To exclude one of the models one needs a process with at least two photons coupling to the quarks, and at least one of these photons has to be real [5]. Quark bremsstrahlung in e^+e^--annihilation fulfills these conditions. Models with integer charged quarks predict a cross section for this reaction which is higher by a factor of ~ 1.75 than the predictions from models assuming fractional charged quarks [5].

The detection of direct photon production is rather complicated, in particular since photons in e^+e^--annihilation can be due to both radiation from the incoming leptons and to a lesser extent from the outgoing charged partons. If a photon is radiated from the initial state, the hadronic state is an eigenstate of the charge conjugation C with $C=-1$, whereas photons emitted from quarks lead to a $C=+1$ state of the hadrons [3]. The interference of these two contributions to the direct photon signal leads to a negative asymmetry in the angular distribution of the positive quark relative to the positive incoming lepton [2]. This charge asymmetry provides therefore evidence for quark bremsstrahlung. A measurement of this charge asymmetry, performed with the TASSO detector at the PETRA storage ring, is reported here. The asymmetry is predicted to be maximum if the photon is radiated with a high transverse momentum relative to the jets as well as to the beam axis [3]. For the measurement of this asymmetry one must select hadronic events with a high energy isolated photon. The isolation of the photon from the jets is essential to reject photons from copiously produced π^0's, which appear in the jets.

2 The detector

A detailed description of the TASSO detector and its lead liquid argon barrel calorimeter can be found elsewhere [6–11]. Because the photon detection is central to this analysis a short description of the barrel lead liquid argon calorimeter is given below. The barrel calorimeter modules are located above and below the magnet coil. They cover 40% of solid angle extending from $42° \leqq \Theta \leqq 138°$ in polar angle in two sections of azimuthal angle, namely $30° \leqq \phi \leqq 150°$ and $210° \leqq \phi \leqq 330°$. They consist of a system of towers and strips. The towers are composed of 2 mm thick lead plates of an area about 7×7 cm^2 (front towers) and about 14×14 cm^2 (back towers) stacked so as to point at the interaction region. Four front towers are followed by one back tower. The strips are about 2 cm wide and etched on copper clad epoxy circuit board. They run orthogonal to the beam axis (z=constant) and parallel to it (ϕ=constant). The first active layer of the calorimeter is at a distance of 178 cm from the interaction point. The front towers contain 6.1 radiation lengths of material, the back towers 7.6 radiation lengths. There are 1.3 radiation lengths of material before the first active layer of the calorimeter. The towers provide a measurement of the total energy of electromagnetic showers with a resolution determined from electrons [9] with energy $1 < E < 5$ GeV

$$\sigma_E/E = (0.136/\sqrt{E}) + 0.03 \quad (E \text{ in GeV}).$$

The electronic threshold of the towers corresponds to a energy deposit of about 18 MeV, which is much lower than the threshold used in the trigger. The strips provide a position resolution determined from electrons [9] with energy $1 < E < 5$ GeV

$$\sigma = (0.77/E + 0.53) \text{ cm} \quad (E \text{ in GeV}).$$

The calibration has been carried out with electrons from Bhabha scattering ($e^+e^- \to e^+e^-$) events. The detection efficiency for a single photon has been deter-

mined from EGS Monte Carlo studies [12] to be 50% at 0.055 GeV rising to >90% above 0.160 GeV. The procedure to combine energy deposits in towers and strips into clusters and the conditions to accept a cluster as produced by a photon have been described recently [11].

3 Analysis

The process to be investigated is, on the parton level,

$e^+ e^- \to q\bar{q}\gamma$.

The photon can come from initial state or final state bremsstrahlung. The presence of final state (quark-)bremsstrahlung will show itself by a forward-backward asymmetry of the positively charged quark w.r.t. the incoming positron direction. We therefore have to select hadronic events with a direct photon, to reconstruct the direction of the quarks by their jet axis and to identify the sign of the charge of the quark from its fragmentation products.

3.1 The event selection

The data were taken between 1981 and 1986. The beam energies varied from 7 GeV up to 23.2 GeV. The integrated luminosity is 205 pb^{-1}, with 175 pb^{-1} taken at beam energies around 17.5 GeV.

In addition to the standard cuts used at TASSO to select multihadron events [13, 14] at least one photon candidate with energy E_γ in the barrel calorimeter is required with:

$0.15\, E_{\text{beam}} < E_\gamma < 0.80\, E_{\text{beam}}$.

From about 63000 multihadron events, 6438 were found which satisfied this criterion.

To select candidates for fully reconstructed hadronic events with an isolated hard photon coming from either initial or final state bremsstrahlung the following conditions are required:

1. $|\cos \Theta_{jet}| < 0.87$, where Θ_{jet} is the angle between the beam and the jet axis (defined below).
2. $p_T > 2.0$ GeV/c, where p_T is the transverse momentum of the photon relative to the nearest jet axis.
3. The sum of the momenta of all charged tracks in a cone of 30° half opening angle around the photon direction has to be smaller than 500 MeV/c. This isolation cut reduces the fraction of non direct photons, produced in a third jet.
4. There is no other photon in the calorimeter, which together with the candidate can form a π^0 with an invariant mass in the range: $100\ \text{MeV/c}^2 < m_{\gamma\gamma} < 180\ \text{MeV/c}^2$.
5. The width of the photon shower, as determined by the strips of the liquid argon calorimater, has to agree with the width produced by a single photon [11]. This discriminates against showers from π^0 decays, where the angle between the two photons is so small that they hit the same front tower and will create one cluster. However, the mean dispersion of the distribution of the fired strips weighted by their energy is significantly larger for overlapping showers than the dispersion created by a single photon of the same energy, providing a means of discrimination.

These cuts are chosen as a result of extensive studies with a Monte Carlo program, that simulates the detector in great detail. The events were generated for the process $e^+ e^- \to q\bar{q}$ and $e^+ e^- \to q\bar{q}g$ according to first order QCD [15] using Field Feynmann fragmentation functions [16]. Initial state radiative effects are included [17]. The response of the calorimeter is simulated with the help of EGS [12]. The shower development of hadrons has also been simulated [18, 19]. After the event generation and detector simulation all events were reconstructed and analysed with the same programs as the data. Since the contribution from quark bremsstrahlung is very small, the event reduction due to the cuts 1–5 is well described by this simulation. Averaged over two methods to reconstruct the jets, as described below, we find that 97% of the events from data and 97.5% of the events from the simulation are rejected by the conditions 1–5.

3.2 The reconstruction of the quark axes

To determine the axes of the primary quarks two methods are used.

Both assume that the events are two jet events and that the photon candidate is a direct photon from initial or final state bremsstrahlung.

Method 1. In the first method the photon four vector is used to boost all charged tracks into the $q\bar{q}$ C.M. system, in which the sphericity axis is determined and used as quark axis. After calculating the jet charge as described in the next section the jet axis is boosted back into the laboratory system under the assumption of massless quarks. For jet momentum, used for the charge estimation, we take the beam momentum minus half of the photon momentum for both jets.

Method 2. The idea of the second method is to look for clusters of charged tracks as preliminary quark axes, combining all charged tracks in a cone of 50° half opening angle around the fastest one into the first cluster. This procedure is repeated with the remaining next fastest track until the fastest remaining

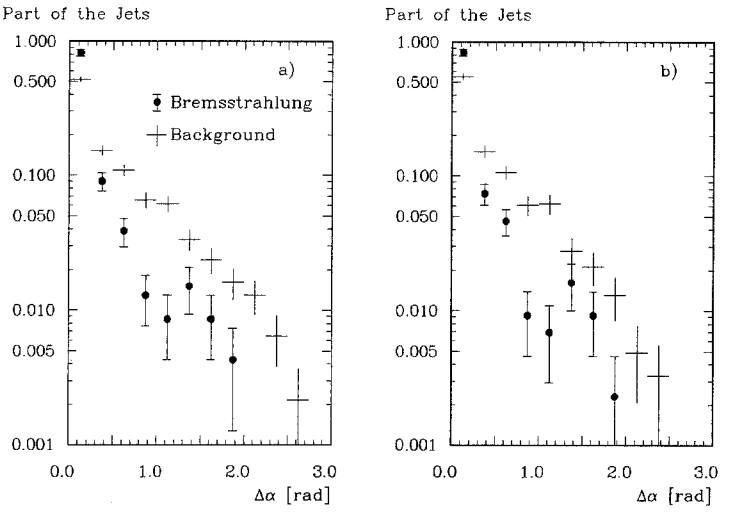

Fig. 1a, b. Difference of angle $\Delta\alpha$ between the true and the reconstructed quark axes.
a Quark axes calculated with the sphericity axis in the $q\bar{q}$ center of mass system (method 1).
b Quark axes from a fit in the laboratory system (method 2)

particle has a momentum below 1 GeV/c. Events with less than two clusters are rejected. The directions of the first two clusters and the photon energy are the inputs for a fit of the angles between the jets and the photon, using the equations of energy and momentum conservation as a constraint and assuming the partons to be massless. The outputs of the fit are two angles and the photon energy. The directions and the energies of the two jets are then determined, up to a rotation around the photon direction. This rotation will be performed in such a way that the angular difference in space between the preliminary and final direction of the first jet is a minimum. If the event has more than two clusters, the first one (belonging to the highest energy jet) is successively taken in combination with all others, and the fit with the smallest χ^2 is used. If the best χ^2 exceeds 4 the event is rejected.

Figure 1a, b shows Monte Carlo predictions of the angular difference in space between the true and the reconstructed quark axes. For these plots we used all events that fulfill the conditions 1–3 as described above. Events where the photon comes from bremsstrahlung and those where it comes from other sources (background) are plotted separately. Both methods lead to similar results and in both cases the quarks axes are significantly better reconstructed if the photon is caused by bremsstrahlung as assumed in the algorithms. Because each event has two true and two reconstructed jets, the assignment between them is made in such a way that the sum of the angular differences between the true and the reconstructed jets is a minimum. For more than 80% of the jets the angular difference in space between the true and the reconstructed jet direction is smaller than 15°. Only less than 1% of the reconstructed jets have an angular difference above 90°.

3.3 Reconstruction of the qark charge

To decide which one of the two jets contains the positively charged quark a jet charge Q_J is determined as suggested first by Field and Feynman [16].

$$Q_J = \sum q_i x_i^\alpha$$

where the sum runs over the charges q_i of all charged particles of the jet with weights x_i^α where x_i is the ratio of the momentum carried by the i^{th} particle and the reconstructed jet momentum. The jet with the larger charge is defined as the positive one. This procedure is motivated by the idea that the charge of the primary parton should be carried by the fastest particles of the jet. Some experimental evidence for this idea has been found [20–24].

Monte Carlo studies showed that, independent of the fragmentation model used [16, 25, 26], the choice of $\alpha = 0.5$ lies at the maximum in the probability p to correctly identify the hemisphere of the positively charged quark though the probability varies only slowly for $0 \leqq \alpha \leqq 1$. This probability differs for the different flavours, with a maximum for the u-quark. Furthermore p depends on the polar angle of the jet axis. If the jet axis lies near the beam axis p decreases by loss of particles due to the limited acceptance of the detector. In the case of a jet axis perpendicular to the beam, p becomes small, because very small errors in the direction of the jet axis can lead to a wrong assignment of the axis to the hemisphere (Figs. 2 and 3). Averaging over all these effects, we found a value of $p = 0.70 \pm 0.04$ for the mean probability to identify correctly the hemisphere of the positively charged quark of those events that fulfill the conditions 1–3 and have a real bremsstrahlung photon. This value of p is obtained from Monte Carlo studies using the fragmentation model of Field and Feynman

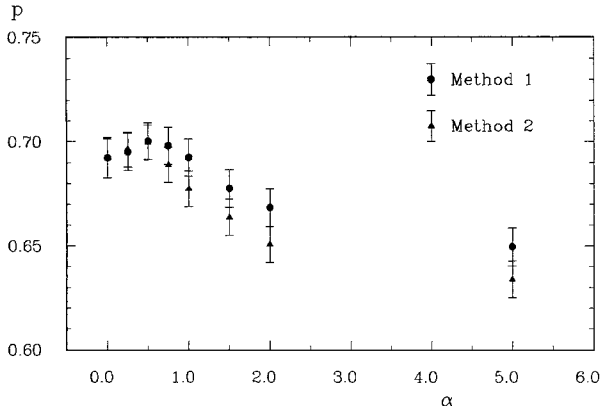

Fig. 2. Average probability p to determine the hemisphere of the positive jet correctly as function of the exponent α of the momentum weight

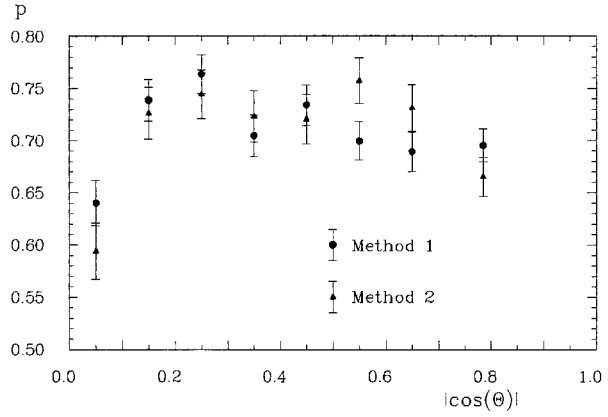

Fig. 3. Probability p to detect the hemisphere of the positive jet correctly vs. the polar angle of the jet axis

[16] as well as from the Lund string fragmentation model [25, 26] and for both algorithms used to estimate the jet axes. To demonstrate that our Monte Carlo simulations describe the jets, their charges and the correlations of the charges correctly, Figs. 4a, b shows the distributions of the product $Q_{J_1} \cdot Q_{J_2}$ of the two jet charges from the Monte Carlo simulation in comparison with the jets of all 6438 multihadron events with a hard photon. The distributions agree over three orders of magnitude.

4 Background

After the cuts 1–5 there remain 205 events with 206 isolated photons from method 1 and 165 events with one photon each from method 2. These photons are mostly caused by bremsstrahlung, but there is a background mainly due to overlapping showers from high energetic π^0 decays. To estimate the fraction of events where the photon is caused by bremsstrahlung a procedure is used, which is nearly independent of the event generator and the fragmentation scheme. It depends on the possibility to distinguish electromagnetic showers caused by single photons from those caused by background. Therefore it needs a precise simulation of the calorimeter. Starting with simulated events passing the cuts 1–3 on the event topology, the probability to accept a single photon by applying the cuts 4 and 5 is determined in addition to the probability to accept a cluster, which is not caused by a single photon. With these two probabilities and the reduction rate due to the cuts 4 and 5 in the

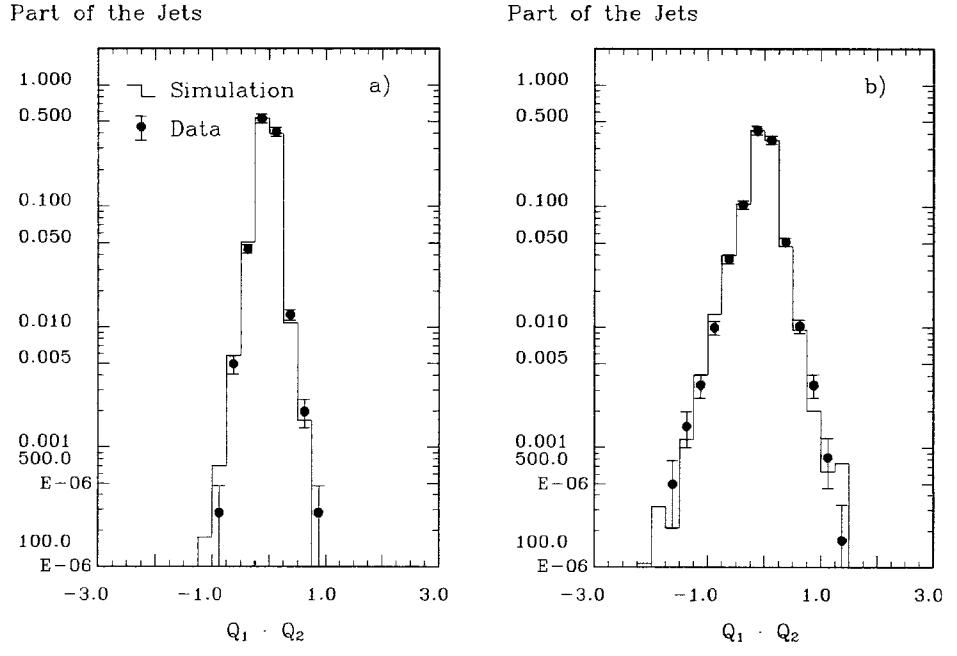

Fig. 4a, b. Distribution of the product of the jet charges from data and simulation.
a Quark axes calculated with the sphericity axis in the $q\bar{q}$ center of mass system (method 1).
b Quark axes from a fit in the laboratory system (method 2)

data, the real number of single photons in the data is evaluated [27]. Averaging over both methods of estimating the jet axes it is found that in $(81.0 \pm 3.3$ (stat.) ± 6.6 (syst.))% of the events the photon is caused by bremsstrahlung. About one half of the remaining background comes from undetected π^0 decays, the rest is shared by photons from η decays and by clusters from other background particles.

5 Results

5.1 Asymmetry

The events passing the cuts 1–5 show a strong forward-backward asymmetry A_γ of the positive jet. With

$$A_\gamma = \frac{N_F - N_B}{N_F + N_B} \tag{1}$$

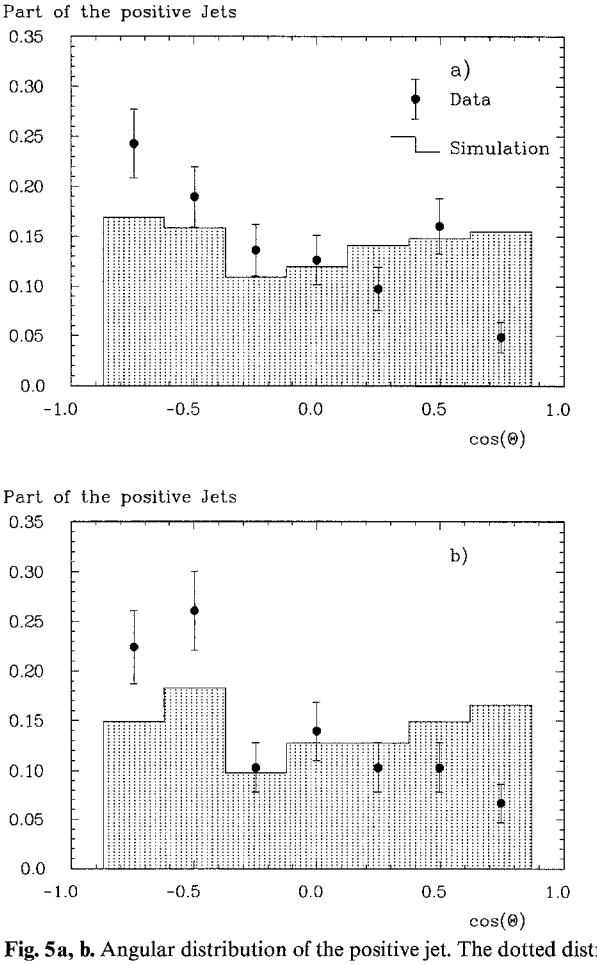

Fig. 5a, b. Angular distribution of the positive jet. The dotted distribution is predicted by a Monte Carlo simulation that contains only initial state radiation. **a** Quark axes calculated with the sphericity axis in the $q\bar{q}$ center of mass system (method 1). **b** Quark axes from a fit in the laboratory system (method 2)

N_F = number of positive jets with an angle $< \pi/2$ relative to the incident positron momentum

N_B = number of positive jets with an angle $> \pi/2$ relative to the incident positron momentum

we find: $A_\gamma = -0.301 \pm 0.067$ (*method* 1, 205 *events*) and $A_\gamma = -0.333 \pm 0.073$ (*method* 2, 165 *events*).

Figure 5a, b shows the measured angular distribution of the positive jet in comparison with a Monte Carlo prediction that includes only initial state radiation.

Averaging both results one gets for the measured asymmetry:
$A_\gamma^{\mathrm{DATA}} = -0.32 \pm 0.07$ (stat.).

Under the assumption of a symmetrically distributed background, the 'background corrected' asymmetry is:

$A_{q\bar{q}\gamma}^{\mathrm{DATA}} = -0.39 \pm 0.09$ (stat.) ± 0.03 (syst.).

5.2 Systematic effects

Z^0 exchange in the quark pair production is expected to create also a genuine charge asymmetry, but the effect is small because the annihilation energy is diminished by initial state radiation and because the contributions to the asymmetry from charge 2/3 and $-1/3$ quarks have opposite signs. As a systematic check of this effect and of our charge identification algorithm the very small positive asymmetry of all multihadron events caused by the electro-weak interference was measured, as reported below. We found that the electroweak contribution to the asymmetry due to the interference of initial and final state bremsstrahlung is below 3% and can be neglected here.

The programs that reconstruct the tracks and the direction of the positive jet are symmetric with respect to the particle charges and should not cause any asymmetry. In order to check this, a sample of simulated events containing no electromagnetic nor electroweak interference has been analysed with the same programs. The found asymmetry is: $A_\gamma^{\mathrm{MC}} = +0.018 \pm 0.065$, which is compatible with zero as expected.

To check for asymmetries of the detector itself μ-pair events and low energetic two-photon events were investigated. No effect was seen [28].

5.3 Comparison with theoretical predictions

To compare the results with theoretical predictions we used a Monte Carlo program by Berends et al. [29, 30] that simulates the process $e^+ e^- \to q\bar{q}\gamma$. This program includes initial and final state radiation as well as their interference, but it assumes massless quarks and does not contain any QCD corrections.

Because of the enormous amount of CPU-time that is necessary to simulate the calorimeter with EGS, the events generated with this program were only passed through the inner detector simulation. The asymmetry from these events, which fulfill the conditions 1–3 as described above and where the photon is known to be from bremsstrahlung, is determined in the same way as for the data. We found:

$A_{q\bar{q}\gamma}^{MC} = -0.153 \pm 0.011$ (*stat.*).

This value has to be compared with the 'background corrected' asymmetry $A_{q\bar{q}\gamma}$. There is a difference between the measured and expected value of the asymmetry of about 2.4 standard deviations, which could be caused by fluctuation of the asymmetry itself or by a fluctuation of the probability to detect the positive jet correctly. Although it is expected that QCD effects do not influence the asymmetry significantly [3], there is no simulation program available yet to study these effects. The asymmetry of the positive quark at the parton level, predicted by the Monte Carlo program used, is for these events -0.357 ± 0.010 (stat.).

5.4 *Comparison with other experiments*

The MAC [31] and JADE [32] collaborations and Gold in his thesis at Mark II [33] also searched for this asymmetry. Because of the very complicated dependencies of this asymmetry on the polar angle and the experimental cuts used, one can only compare the measured asymmetries with their Monte Carlo predictions. For all measurements the Monte Carlo program from Berends et al. was used [29, 30]. The results are summarized in Table 1. Because all other experiments did not correct for their remaining background, one has to compare them with our measured asymmetry A_γ. For the comparison of the Monte Carlo predictions we added to our Monte Carlo prediction of $A_{q\bar{q}\gamma}$ a symmetrically distributed background of 19% as determined from the data, which leads to $A_\gamma^{MC} = -0.12 \pm 0.015$.

Only the result from [33], where the analysis was performed with similar cuts and a comparable number of events, can be directly compared, and is consistent with our results within the errors.

Table 1. Comparison of the measured and predicted asymmetries of different experiments

Experiment	Measured asymmetry	Predicted asymmetry
MAC	-0.123 ± 0.035	-0.117 ± 0.026
JADE	-0.06 ± 0.07	-0.14 ± 0.05
M.S. Gold (Mark II)	-0.246 ± 0.055	-0.231 ± 0.06

5.5 *The cross section*

For the determination of the cross section only data are used with 15 GeV $< E_{beam} <$ 18 GeV. The integrated liminosity of this event sample is 175 pb^{-1}. All other cuts have been applied as described. In addition a correction for inefficiencies in the liquid argon calorimeter was applied (factor 1.05 ± 0.03). The background is calculated as described above. Note that the Monte Carlo calculation used for the background subtraction does not include final state bremsstrahlung. The excess number of photons in the data compared to this Monte Carlo is 38.6 ± 13.1 (stat.)-± 11.5 (syst.), which we attribute to final state bremsstrahlung. Figure 6 shows the acceptance corrected cross section for the reaction $e^+ e^- \to q\bar{q}\gamma$. The prediction of a simulation program including also final state bremsstrahlung according to [29, 30] overestimates the cross section slightly. The contribution from initial state radiation predicted by this program is also plotted. It has been shown that QCD effects, which are not included in this program, should lower the cross section by ~25% [3]. The cross section from the Monte Carlo [29, 30], decreased by 25%, describes the data reasonably. Models with integer charged quarks predict a cross section for quark

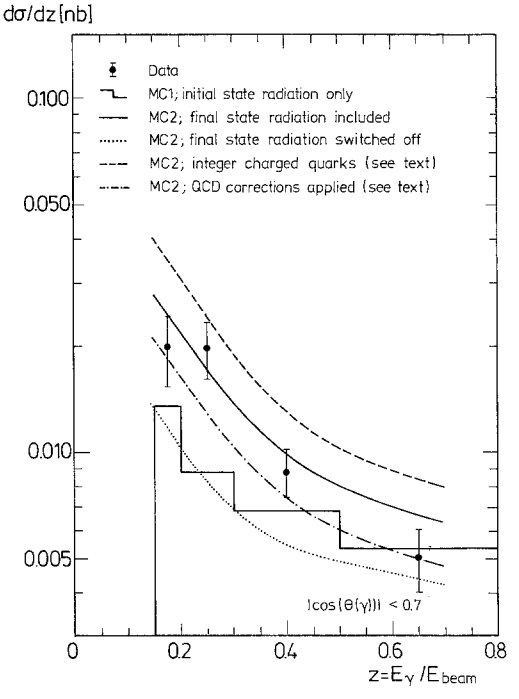

Fig. 6. Cross section $d\sigma/dx$ for the reaction $e^+ e^- \to q\bar{q}\gamma$. The indicated errors are statistical only

Table 2. Systematic errors on the cross section

$x=E_\gamma/E_{\text{beam}}$	0.15–0.20	0.20–0.3	0.3–0.5	0.5–0.8
Source of error	$\Delta\sigma/\sigma$ [%]			
Efficiency	5.0	5.0	5.0	5.0
Background	16.8	11.0	6.3	7.4
Acceptance	20.0	20.0	20.0	20.0
Luminosity	3.6	3.6	3.6	3.6
$\sqrt{\sum\left(\frac{\Delta\sigma}{\sigma}\right)^2}$	26.8	23.6	21.9	22.2

bremsstrahlung, which is higher by a factor of ~ 1.75 than the cross section predicted by models assuming fractional charged quarks [5]. Multiplying the final state component of the cross section from simulation program [29, 30] by 1.75 leads to a clear overestimate of the cross section. The plot contains the statistical errors only and the systematic errors are of the order of 25%. In Table 2 the contributions to the systematic error are summarized. The final error is estimated by adding all contributions in quadrature.

6 The inclusive electroweak asymmetry

The cross section for fermion pair production in the standard model has the following form [34–37]:

$$\frac{d\sigma}{d\Omega}=\frac{\alpha^2}{4s}\left[A(1+\cos^2\Theta)+B\cos\Theta\right]$$

$$A=Q_f^2-2Q_f v v_f \operatorname{Re}(\chi)+(v^2+a^2)(v^2{}_f+a_f^2)|\chi|^2$$

$$B=4(-Q_f a a_f \operatorname{Re}(\chi)+2v a v_f a_f|\chi|^2)$$

$$\chi=\frac{1}{4\sin^2 2\Theta_W}\frac{s}{s-M_Z^2+iM_Z\Gamma_Z}. \qquad (2)$$

The index f marks the outgoing fermions of the final state, Θ is the angle between the electron and the outgoing fermion, v and a are the vector and axial vector coupling constants, M_Z and Γ_Z denote the mass and width of the Z^0, Θ_W is the Weinberg angle and Q is the electric charge.

A measurement of the inclusive charge asymmetry in all hadronic events does not distinguish between quarks and antiquarks, therefore the contributions from the positive charged u and c quarks and from the negative charged d, s and b quark partly cancel.

This measurement is useful as a check for instrumental asymmetries and for the charge identification algorithm. Since the majority of these events do not have a hard bremsstrahlung photon, one expects no measurable contribution of the asymmetry from the interference of initial and final state bremsstrahlung.

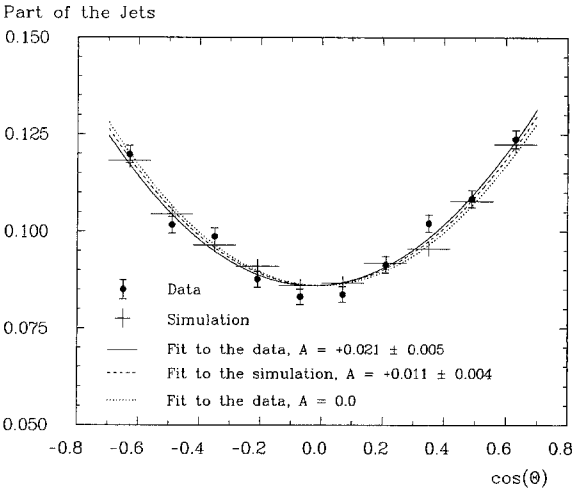

Fig. 7. Angular distribution of the positive jet for all multihadron events. The distribution is corrected for acceptance and radiative effects

We used hadronic events with 15 GeV $< E_{\text{beam}} <$ 18 GeV. The sphericity axis has been used as a quark axis. For the polar angle of the sphericity axis we required: $|\cos\Theta_{\text{sph}}|<0.7$ and the value of the sphericity had to lie below 0.25, to reject three jet events. These conditions are fulfilled by 33458 events. Using a maximum likelihood fit with the function:

$$f(\cos\Theta)=C(\tfrac{3}{8}(1+\cos^2\Theta)+A\cos\Theta)$$

C : Normalisation

A : Asymmetry

as predicted by the standard model, the inclusive electroweak asymmetry is measured to be:

$$A^{\text{ew.}}_{\text{meas.}}=+0.021\pm0.005 \quad (Data)$$

which is somewhat larger than predicted by a Monte Carlo simulation using the Lund 4.3 geneator and the standard model [25, 26] (Fig. 7) including QCD corrections up to the order α_s^2 and assuming massive quarks with $m_u=m_d=0.3$ GeV/c^2, $m_s=0.5$ GeV/c^2, $m_c=1.5$ GeV/c^2 and $m_b=5.0$ GeV/c^2: $A^{\text{ew.}}_{\text{sim.}}=+0.011\pm0.004$. On the parton level the Monte Carlo program predicts for these events according to the standard model an asymmetry of the positively charged quark of: $A^{\text{ew.}}_{\text{parton}}=+0.024\pm0.004$.

The difference between the data and the prediction becomes smaller if one uses a jet charge determination requiring the reconstructed charges of the jets to have opposite sign. This reduces the data sample to 18992 events and the asymmetry becomes $A^{\text{ew.}}_{\text{meas.}}=+0.026\pm0.007$ which has to be compared with $A^{\text{ew.}}_{\text{sim.}}=+0.018\pm0.006$ from the simulation. A similar measurement was presented by the MAC collaboration

[38]. They found: $A_{\text{meas.}}^{\text{ew.}} = +0.028 \pm 0.005$ in agreement with their Monte Carlo prediction of $+0.022$. Also in a thesis at the JADE collaboration a similar value was reported [39].

7 Conclusion

In hadronic events from $e^+ e^-$-annihilation with an isolated high energy photon a significant forward-backward asymmetry A_γ of the positively charged jet with respect to the incident positron direction has been found: $A_\gamma = -0.32 \pm 0.07$, providing evidence for photon bremsstrahlung from quarks.

The cross section for emission of high energy photons in the reaction $e^+ e^- \to q\bar{q}\gamma$ is in agreement with theoretical predictions assuming fractional charged quarks if quark bremsstrahlung is included. A final exclusion of models with integer charged quarks is not possible, but they are disfavoured by this measurement.

As a check of the charge identification algorithm the inclusive forward-backward asymmetry of all hadronic events at C.M. energies between 30 GeV and 36 GeV has been measured and found to be compatible with theoretical expectations. Corrected for the limited acceptance of the detector we found: $A = +0.021 \pm 0.005$.

Acknowledgements. We gratefully acknowledge the support of the DESY directorate, the PETRA machine group and the staff of the DESY computer center. Those of us from outside DESY wish to thank the DESY directorate for the hospitality extended to us.

References

1. T.F. Walsh, P.M. Zerwas: Phys. Lett. **44 B** (1973) 195
2. S.J. Brodsky, C.E. Carlson, R. Suaya: Phys. Rev. **D 14** (1976) 2264
3. E. Laermann, T.F. Walsh, I. Schmitt, P.M. Zerwas: Nucl. Phys. **B 207** (1982) 205
4. M.Y. Han, Y. Nambu: Phys. Rev. **138** (1965) 1006
5. T. Jayaraman, G. Rajasekaran, S.D. Rindani: Phys. Rev. **D 32** (1985) 1262
6. TASSO Coll. R. Brandelik et al.: Phys. Lett. **108 B** (1982) 71
7. TASSO Coll. R. Brandelik et al.: Phys. Lett. **83 B** (1979) 261
8. TASSO Coll. R. Brandelik et al.: Phys. Lett. **94 B** (1980) 437
9. TASSO Coll. M. Althoff et al.: Phys. Lett. **146 B** (1985) 443
10. TASSO Coll. M. Althoff et al.: Z. Phys. C – Particles and Fields **26** (1984) 337
11. TASSO Coll. W. Braunschweig et al.: Z. Phys. C – Particles and Fields **33** (1986) 13
12. R. L. Ford, W.R. Nelson: SLAC Report 265, UC-32 (1985)
13. TASSO Coll. R. Brandelik et al.: Phys. Lett. **113 B** (1982) 499
14. TASSO Coll. R. Brandelik et al.: Phys. Lett. **114 B** (1982) 65
15. P. Hoyer et al.: Nucl. Phys. **B 161** (1979) 349
16. R.D. Field, R.P. Feynman: Nucl. Phys. **B 136** (1978) 1
17. F.A. Berends, R. Kleiss: Nucl. Phys. **B 178** (1981) 141
18. A. Grant: Nucl. Instrum. Methods **131** (1975) 167
19. H. Fesefeldt: Aachen PITHA Report 85–02
20. TASSO Coll. R. Brandelik et al.: Phys. Lett. **100 B** (1981) 117
21. PLUTO Coll. Ch. Berger et al.: Nucl. Phys. **B 124** (1983) 189
22. CLEO Coll. S. Berends et al.: Phys. Rev. **D 31** (1985) 2161
23. HRS Coll. M. Derrick et al.: Phys. Rev. Lett. **54** (1985) 2568
24. TASSO Coll. M. Althoff et al.: Z. Phys. C – Particles and Fields **29** (1985) 347
25. T. Sjöstrand: Comput. Phys. Commun. **27** (1982) 243
26. T. Sjöstrand: Comput. Phys. Commun. **28** (1983) 229
27. W. Zeuner: Dissertation, Hamburg (1988) and DESY Internal Report F35D-88-01
28. TASSO Coll. R. Brandelik et al.: Phys. Lett. **110 B** (1982) 173
29. F.A. Berends, R. Kleiss, S. Jadach: Nucl. Phys. **B 202** (1982) 63
30. F.A. Berends, R. Kleiss, S. Jadach: Comput. Phys. Commun. **29** (1983) 185
31. MAC Coll. E. Fernandez et al.: Phys. Rev. Lett. **54** (1985) 95
32. JADE Coll. W. Bartel et al.: Z. Phys. C – Particles and Fields **28** (1985) 343
33. M.S. Gold: Ph.D. Thesis, Berkeley, LBL-22433 (1986)
34. S. Weinberg: Phys. Rev. Lett. **19** (1967) 1264
35. A. Salam: Proceedings of the 8th Nobel Symposium. N. Svartholm (ed.), p. 367. Stockholm: Almquist and Wiksells 1968
36. R. Budny: Phys. Lett. **55 B** (1975) 227
37. Proceedings of the 1975 PEP summer study, LBL-4800/SLAC-190, p. 31.
38. MAC Coll. E. Fernandez et al.: Phys. Rev. Lett. **58** (1987) 1080
39. P. Warming, Ph.D. Thesis, Hamburg (1987)